PAPER • **OPEN ACCESS**

Numerical investigation of turbulent fuel jet diffusion and its influence on the auto-igniting diffusive flame development

Journal of Physics: Conference Series **2893** (2024) 012032 doi:10.1088/1742-6596/2893/1/012032

Numerical investigation of turbulent fuel jet diffusion and its influence on the auto-igniting diffusive flame development

Carlo Cravero[1*], Alessandro Lamberti[1], Davide Marsano[1], Gabriele Milanese[1]

[1] Dipartimento di Ingegneria Meccanica, Energetica, Gestionale e dei Trasporti, Università degli Studi di Genova , Genoa , Italy

[*]E-mail: cravero@unige.it, alessandro.lamberti@edu.unige.it, davide.marsano@unige.it, gabriele.milanese@unige.it

Abstract. Turbulent auto-igniting diffusion flames are common in combustion systems, where the mixing of the fuel jet with the outer oxidant flow is the fundamental mechanism for the flame ignition and development. The paper presents a critical analysis on the Reynolds-Averaged-Navier-Stokes (RANS) simulation of a methane-air flame, done with a two equations turbulence model, in comparison with detailed experimental data. In the first part, the non-reactive jet is simulated with the standard $k-\varepsilon$ model and a modified version, obtained with motivated changes of the C_μ and σ_k constants. In the second part the reactive jet is simulated, introducing a consistent modification of the C_γ constant, in the eddy dissipation concept (EDC) model. The comparison with experimental data confirms the validity of the proposed model and highlights the effect of the proper turbulent jet development on the mechanisms of the diffusive flame ignition and propagation.

1. Introduction

Turbulent auto-igniting diffusion flames are used in many industrial applications (e.g. furnaces [1]). These flames result from the interaction of a turbulent fuel jet with an oxidant at high temperature, leading to spontaneous ignition and flame propagation [2]. Within this context, the simulations accuracy is strongly dependent on the behaviour of the adopted models for turbulent mixing and turbulence-chemistry interaction which, if not carefully validated, can lead to high interacting errors, difficult to be distinguished.

During last years, much work has been dedicated to the RANS simulations of Jets in hot Coflow (JHC), focussing on Moderate or Intense Low Oxygen Dilution (MILD) conditions.

The Adelaide JHC [3] has been studied by Christo and Dally [4], Amiminian et al. [5], Parente et al.[6], Li et al. [7], while the Delft JHC [8] has been analysed by Oldenhof et al. [9], Lewandowski and Ertesvag [10, 11], Labahn et al. [12]. These works, being part of a wider bibliography on the subject, performed an extensive investigation on the influence of the kinetic mechanism, the turbulence-chemistry interaction model and the turbulence model. Despite these efforts, the key aspect of properly modelling the initial region of the turbulent jet development seems to be left open. The experimental work of Cabra et al. [13,14,15], together with the complementary studies of Masri et al. [16] and Gordon et al. [17] provide measurements of species, temperature and velocity, suitable for a clarifying validation study. RANS simulations of the Cabra hydrogen flame have been done by Cabra et al. [14], Masri et al. [18], Cao et al. [19], Gkagkas and Lindstedt [20],

Benin and Pfeiffelman [21], while the methane-air flame has been studied by Cabra et al. [15] and Gkagkas and Lindstedt [22].

In the present work, RANS simulations of the Cabra methane-air case, are carried out. The results obtained with the standard $k-\varepsilon$ model, on the non-reactive jet, are critically analysed and a modified version is proposed, with physically motivated changes of the C_μ and σ_k constants. The modified model is satisfactorily tested on the reactive jet, introducing a consistent change in the EDC model. The results can be used to improve the reliability of RANS simulation for industrial applications, providing also a general information for further developments in the simulation of turbulent jets.

2. The burner

The Cabra burner (Figure 1) consists of a central fuel jet nozzle with an inner diameter of 4.57 mm (o.d. 6.35 mm), surrounded by a coaxial flow of hot combustion products (vitiated coflow), issuing from a perforated plate of 210 mm diameter. Gordon et al. [17] used a replica of the Cabra burner with a central nozzle of 4.45 mm inner diameter and a perforated plate of 190 mm.

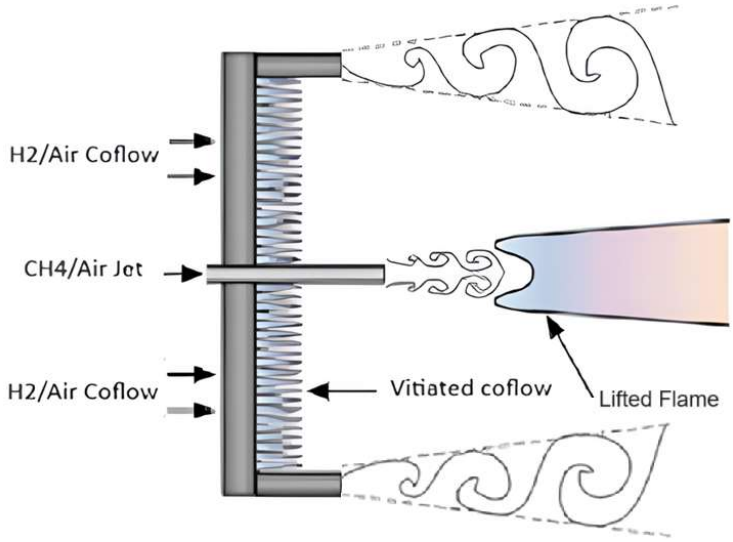

Figure 1. Schematic diagram of the Cabra burner [13].

3 Numerical Model

The simulations are performed using the Finite Volume Method code Ansys Fluent 17.1 [23], with the pressure-based solver and the *Coupled* solution method for the pressure-velocity coupling. The advection terms are discretized with the second order upwind scheme. The chemical kinetic mechanism DRM19 [24] is used, with 19 species and 84 reversible reactions. The Fluent Stiff Chemistry Solver is employed with an Absolute Error Tolerance of $1{\cdot}10^{-8}$ and a Relative Error Tolerance of $1{\cdot}10^{-9}$. The ISAT method is used with the error tolerance set to 0.001, after checking the accuracy with the tolerance reduced by two orders of magnitude. The fluid mixture is treated as incompressible ideal gas, with the thermodynamic and transport properties of each species calculated from the GRIMECH 1.2 dataset [25]. The mixture specific heat, molecular viscosity and thermal conductivity are calculated with the mixing law, while the mass diffusivity is obtained with the kinetic theory. Heat transfer due to radiation is calculated using the P1 model, with the weighted-sum-of-gray-gases model for the absorption coefficient.

The solution convergence is evaluated with the residuals (below 10^{-5} for all the equations) and with monitor points of relevant variables (i.e. temperature, velocity and O2 mole fraction) along the jet axis.

3.1 Turbulence modelling

The two equations k-ε turbulence model is used [26], with the following form :

$$\tau_{ij} = \overline{u_i' u_j'} = 2\nu_T S_{ij} - \frac{2}{3} k \delta_{ij} \tag{1}$$

$$\nu_t = C_\mu \frac{k^2}{\varepsilon} \tag{2}$$

$$\frac{\partial(k)}{\partial t} + U_i \frac{\partial(k)}{\partial x_i} = \frac{\partial}{\partial x_j}\left[(\nu + \frac{\nu_t}{\sigma_k})\frac{\partial k}{\partial x_j}\right] + \tau_{ij}\frac{\partial U_i}{\partial x_j} - \varepsilon \tag{3}$$

$$\frac{\partial(\varepsilon)}{\partial t} + U_i \frac{\partial(\varepsilon)}{\partial x_i} = \frac{\partial}{\partial x_j}\left[(\nu + \frac{\nu_t}{\sigma_\varepsilon})\frac{\partial k}{\partial x_j}\right] + C_{\varepsilon 1}\frac{\varepsilon}{k}\tau_{ij}\frac{\partial U_i}{\partial x_j} - C_{\varepsilon 2}\frac{\varepsilon^2}{k} \tag{4}$$

where $S_{ij} = \frac{1}{2}\left(\frac{\partial U_i}{\partial x_j} + \frac{\partial U_j}{\partial x_i}\right)$ is the strain rate tensor, $k = \frac{1}{2}\overline{u_i' u_i'}$ is the turbulent kinetic energy (TKE) , $\tau_{ij}\frac{\partial U_i}{\partial x_j}$ and ε are respectively the TKE production (P_k) and its dissipation rate.

The standard values of σ_k and σ_ε are 1 and 1.3 respectively, based on two-dimensional shear flows results. $C_{\varepsilon 2}$ is 1.92, evaluated from the decay of isotropic turbulence, $C_{\varepsilon 1}$is 1.44 and C_μ is 0.09, based on the logarithmic region of a fully developed boundary layer [27].

Equation (1), for a 2D shear flow, gives the following relationship between the C_μ value, the shear component $b_{12} = \frac{\overline{u_1' u_2'}}{2k}$ of the anisotropy tensor and the shear parameter $S^* = \frac{\partial u_1}{\partial x_2}\frac{k}{\varepsilon}$:

$$C_\mu = {}^{2b_{12}}/_{S^*} \tag{5}$$

Experimental and numerical works, taking into account contained uncertainties and flow setup dependency, provide the following reference values :

Table 1. C_μ in different flow regimes

Shear intensity	Example	S^*	b_{12}	C_μ	P_k/ε	Reference
Low-medium	Log-law region of fully developed boundary layer (BL)	~3	~0.15	~0.1	1	[28,29]
Medium	Log-law region in flat plate BL	≥ 5	~0.16	~0.05	$1 < P_k/\varepsilon < 2$	[30,31]
High	Overlap region in BL	≥ 10	~0.1	~0.01	≥ 2	[32]

It is well known and widely documented the diffusion excess produced on a turbulent round jet by the standard $k-\varepsilon$, which is usually tackled acting on the turbulent dissipation levels. This is mainly done by modifying the production and destruction terms in the dissipation rate equation [33, 34], tailored on the basis of data related to self-preserving jet region.

This work analyses the influence of the C_μ constant, particularly in the initial region (i.e. jet flow establishment zone) whose behaviour is briefly described. Where the turbulent boundary layer leaves the pipe walls, the shear intensity is high and, relating to Table 1, C_μ can be as low as 0.01. The velocity gradient is then reduced by the shear stress action, leading to a medium shear intensity region, with a corresponding C_μ value below 0.09. These flow features are emphasized by the density difference between the jet and the coflow [35, 36]. Based on these arguments, a compromise value of 0.03 is used for C_μ in the modified $k-\varepsilon$ model, and a σ_k value 0.75 is set to avoid an excessive reduction of turbulent diffusion (Eqs. (2) and (3)). This C_μ modified value aims to simulate accurately the initial zone, considering that, though being too low for the self-similarity zone of a non-reactive jet, it allows the necessary accuracy when the flow is dominated by flame-induced velocity gradients. In the following, the standard $k-\varepsilon$ model is referred to as STD, and the modified version as MOD.

3.2 Turbulence/chemistry interaction

The EDC [37] model is employed to represent the interaction between turbulence and chemical reactions which are assumed to occur inside the small turbulence structures. The volume fraction of the fine scales and the reaction time scale are modelled respectively using the length scale γ^* and the mean residence time τ^*:

$$\gamma^* = C_\gamma \left(\frac{\nu\varepsilon}{k^2}\right)^{1/4} \quad (6) \qquad \tau^* = C_\tau \left(\frac{\nu}{\varepsilon}\right)^{1/2} \quad (7)$$

The mean reaction rate, providing the source-term in the conservation equation for the mean species i, is defined as:

$$R_i = \frac{\rho(\gamma^*)^2}{\tau^*[1-(\gamma^*)^3]}(Y_i^* - Y_i) \quad (8)$$

where Y_i is the mean mass fraction of the species i between the fine structure and the surrounding fluid and Y_i^* is the fine-scale species mass fraction after reacting over the time τ^*. Y_i^* is computed, in the Fluent implementation [23], by integration of a Plug flow Reactor (PFR) using the instantaneous formation rate provided by the kinetic mechanism.
The EDC model constants are defined by the following relations :

$$C_\gamma = \left(\frac{3}{4}\frac{C_{D2}}{C_{D1}^2}\right)^{\frac{1}{4}} \quad (9) \qquad C_\tau = \left(\frac{C_{D2}}{3}\right)^{1/2} \quad (10)$$

The EDC values of C_{D1} and C_{D2} are 0.135 and 0.5 respectively [37, 38].
The C_{D1} value is related to the turbulent viscosity :

$$\nu_t = \frac{2}{3}C_{D1}\frac{k^2}{\varepsilon} = C_\mu\frac{k^2}{\varepsilon} \quad (11)$$

As discussed by Estersvag et al. [37], a change in the turbulence model constants must be accompanied by consistent modifications of the EDC model constants C_γ and C_τ.
Based on Eqs. (9) and (11), a reduction of C_μ has to be followed by a proper variation of C_γ, as analysed in the subsection 4.2.1.

3.3 Computational domain and mesh sensitivity
Figure 2a shows the simulated domain, consisting of an axisymmetric 2D geometry, with the inlet boundary conditions (velocity-inlet) indicated in blue and the outlet conditions in red (pressure-outlet), with a focus on the jet exit zone in Figure 2b.

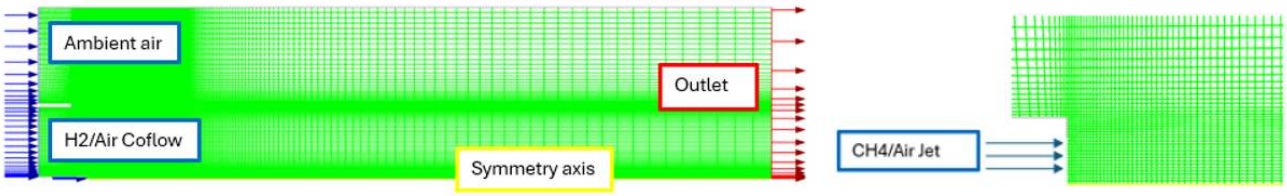

Figure 2. Computational domain: (a) complete domain, (b) Jet focus

The fuel jet boundary conditions (i.e. velocity, turbulence kinetic energy and dissipation profiles) are obtained from an axisymmetric simulation of a fully developed boundary layer in a pipe , validated against DNS data [39]. The simulation is carried out on a 1 m axisymmetric pipe, with a y+ of about 30 for the first cell near the wall. This approach has two advantages: one is to avoid the approximation resulting from using data not measured at the exact jet exit location and not including the TKE dissipation, the second is the possibility to modify the turbulence model constants without compromising the jet exit profile. For the sake of compactness, the results of the pipe simulation are not shown here. All the boundary conditions are summarised in Table 2.

Table 2. Boundary conditions

Name	Type	Velocity [m/s]	Temperature [K]	Pressure [Pa]	Species (mole fractions), sum up to 1 with N2
CH4/Air jet	Velocity-inlet	2D simulation profile	320	-	CH4=0.33, O2=0.15, H2O=0.0029
H2/Air coflow	Velocity-inlet	5.3	1420	-	O2=0.12, H2O=0.15
Outlet	Pressure-outlet	-	300	101325	O2=0.21
Ambient air	Velocity-inlet	0.5	300	-	O2=0.21

For the burner model, a structured mesh is used with a refinement in the exit area of the pipe and along the axis of the fuel jet. In order to assess the mesh independency, simulations are done with 3 meshes having respectively 11000, 30000 and 60000 nodes.

Results of mesh sensitivity study are shown in Figure 3, where the non-dimensional velocity on the jet axis and the distribution along the section at 15 diameters away from the jet exit are shown (U is the velocity magnitude and U_j the average jet velocity). The mesh with 30000 nodes, (460 nodes along the symmetry axis, 15 nodes on the fuel inlet, 60 nodes on the coflow and 30 nodes on the external flow) is used in the following.

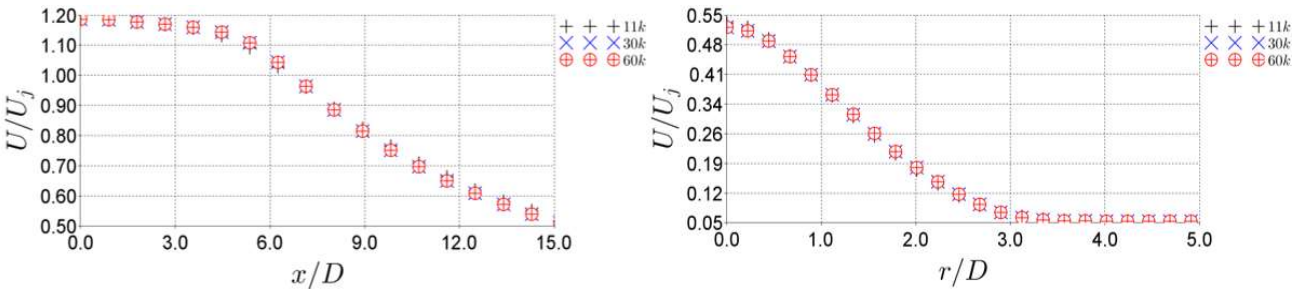

(a) **(b)**

Figure 3. Mesh sensitivity study: (a) axial decay of velocity, (b) velocity distribution at fifteen diameters.

4 Simulation analysis

The simulation campaign is divided into two parts: the first series is dedicated to the simulation of the non-reactive flow, to assess the turbulence model ability to reproduce the main flow features, while in the second series the reactive jet is simulated.

4.1 Non-reactive jet

In this section the simulated velocity and shear stress distributions, taken at different axial positions, are compared with the corresponding measurements [17]. The results are shown in Figures 4 and 5 in dimensionless terms, using the average jet velocity as reference.

With the $k-\varepsilon$ STD, the velocity spreading rate is clearly overestimated, while with the $k-\varepsilon$ MOD there is a reasonable agreement with the experimental data. This behaviour can be understood, in the light of the above subsection 3.1, analysing the evolution of the shear stress distribution (Fig. 5a) and of the TKE production (Fig. 6a). In Fig. 5a the $k-\varepsilon$ STD C_μ value gives a high narrow peak of the shear stress (not resolved by measurements) which, in turn, is responsible for a strong local TKE production (Fig. 6a). As a consequence, an excess of turbulent diffusion is produced which, at the downstream locations, leads to shear stress profiles greatly overestimated and shifted. This behaviour is still evident at 40 diameters, where, for the reactive case, the flame evolution is expected to be significantly impacted.

With the $k-\varepsilon$ MOD, the initial peaks of the shear stress (Fig. 5b) and of the consequent TKE production (Fig. 6b) are mitigated, leading to a much better agreement with the experimental data. Consequently, it can be inferred that the $k-\varepsilon$ MOD provides a good basis on which the flame structure can be modeled with higher coherence.

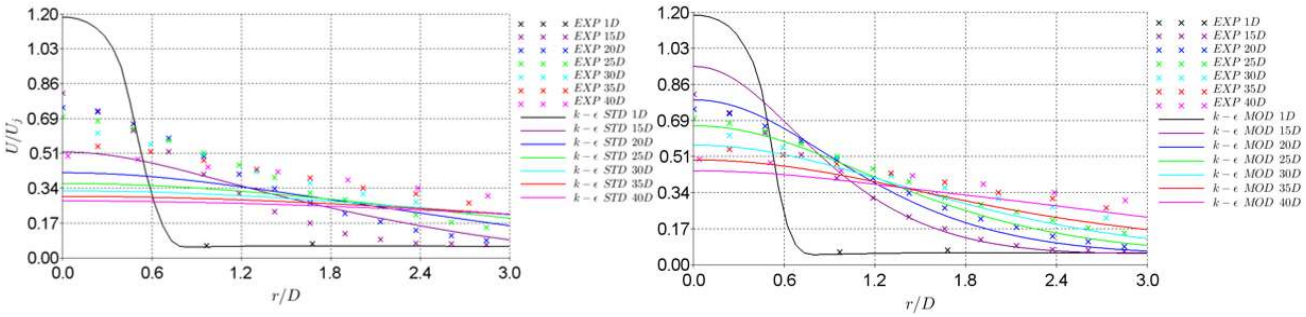

(a) **(b)**

Figure 4. Dimensionless velocity profiles: (a) $k-\varepsilon$ STD, $k-\varepsilon$ MOD

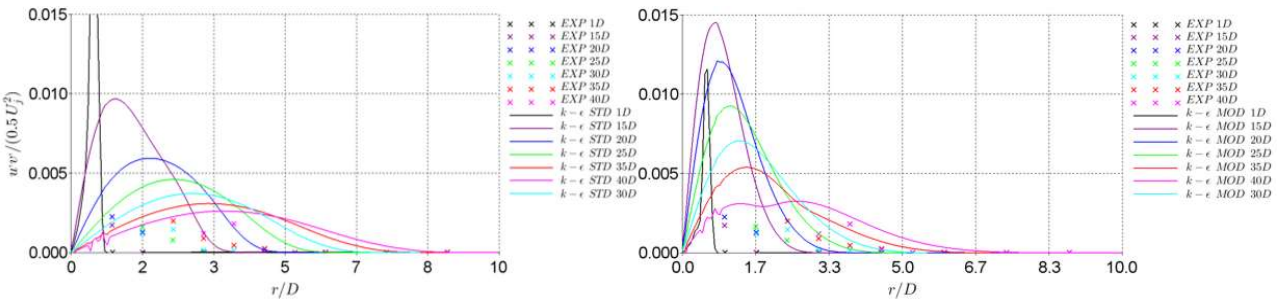

(a) **(b)**

Figure 5. Dimensionless Reynolds tangential stress profiles: (a) $k-\varepsilon$ STD, (b) $k-\varepsilon$ MOD

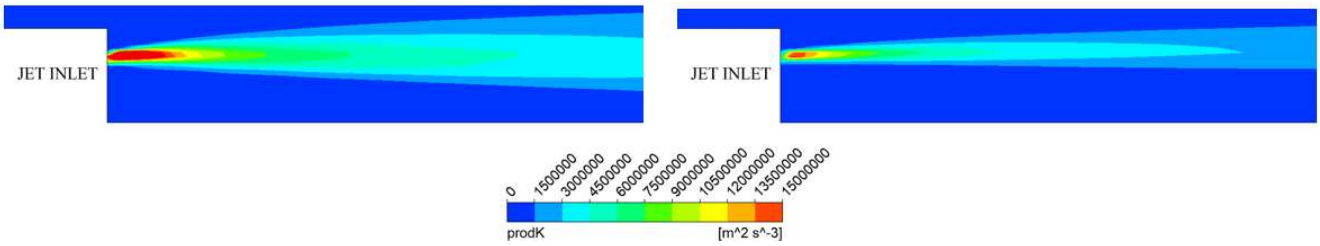

(a) **(b)**

Figure 6. Turbulence kinetic energy production contours: (a) $k-\varepsilon$ STD, (b) $k-\varepsilon$ MOD

4.2 Reactive jet

The following set of simulations involves the use of the chemical kinetic mechanism DRM19 and the EDC turbulence chemistry interaction model. Notably, the experimental data pertaining to the reactive flow are available up to 70 diameters from the fuel exit, thus enabling a comprehensive analysis of the flow and flame structure and their respective responses to the turbulence model.

Results of the reactive jet with the STD and the MOD version of $k-\varepsilon$ are shown in Figures 7 and 8, regarding the temperature and CO2 mass fraction profiles. With the $k-\varepsilon$ STD an early flame ignition is produced, shown by temperature and CO2 mass fraction peaks at 30 diameters. Then, a too large flame radial development is evident. As expected, the $k-\varepsilon$ MOD with the default EDC constants leads to a late ignition, due to a lower reaction rate.

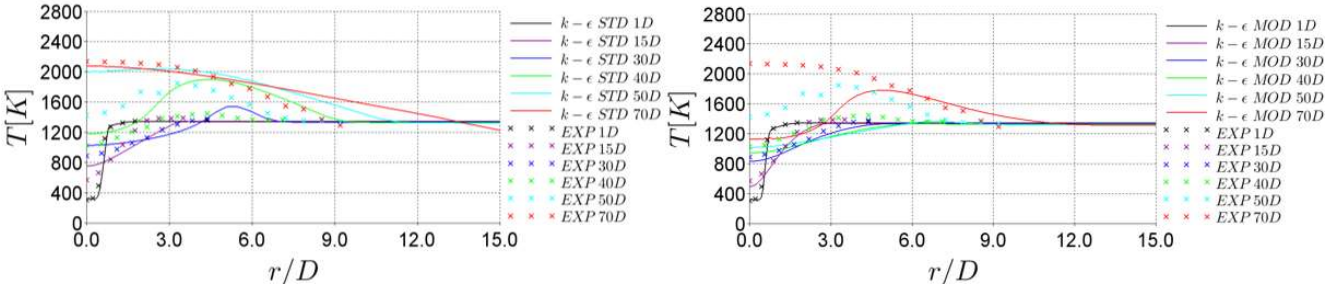

(a) **(b)**

Figure 7. Temperature profiles in reactive jet: (a) $k-\varepsilon$ STD, (b) $k-\varepsilon$ MOD.

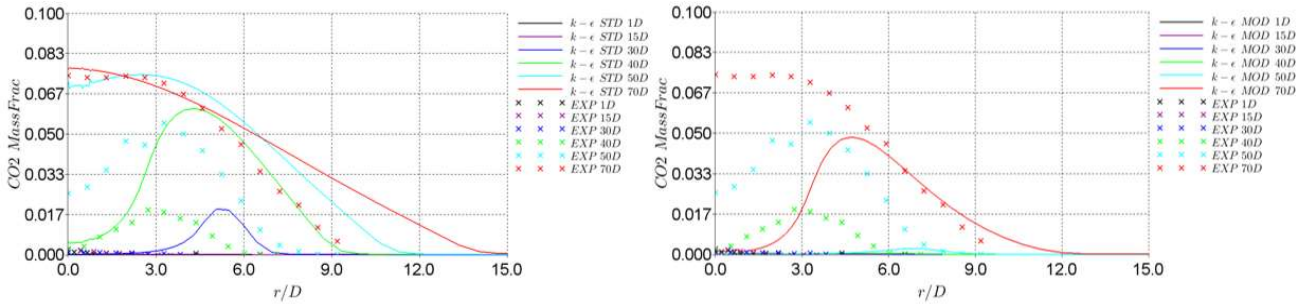

(a) **(b)**

Figure 8. CO2 Mass fraction profiles: (a) $k-\varepsilon$ STD, (b) $k-\varepsilon$ MOD.

4.2.1 Simulations with modified EDC

In this section, we show the results obtained with the EDC model, modified following the analysis of the subsection 3.2. Strictly applying Eqs. (9) and (11), a C_μ value of 0.03 implies a C_γ value of 3.69, significantly higher than the default value of 2.1377 [37,38].

Since the C_μ reduction affects in a complex way the k and ε distributions, entering the fine turbulent length scale in Eq. (6), a better C_γ value can be obtained from a sensitivity analysis, based on simulation results. For this purpose, simulations are carried out with C_γ values of 3.69, 3, 2.5 and 2.3, giving respectively an ignition point located at 15 (for the first two $C_\gamma$values), 40 and 50 diameters away from the jet exit. The detailed results obtained with C_γ 3.69 ($k-\varepsilon$ MODA) and 2.3 ($k-\varepsilon$ MODB) are presented in Figures 9 and 10.

In Figures 9a and 10a, the temperature and CO2 profiles, for $k-\varepsilon$ MODA, show an early flame ignition point and consequent flame development. The $k-\varepsilon$ MODB (Fig. 9b and 10b), with a C_γ value slightly higher than the default, shows an ignition point and a flame development more consistent with the experiment, at around 50 diameters from the jet exit.

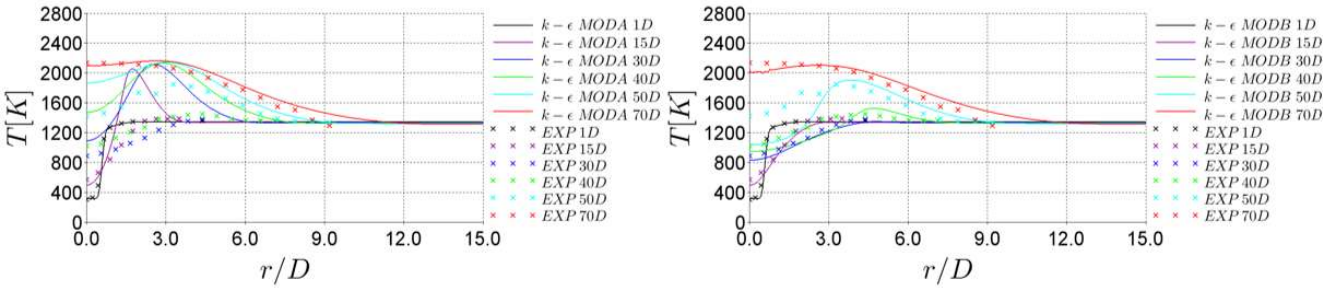

(a) **(b)**

Figure 9. Temperature profiles of modified EDC models: (a) $k-\varepsilon$ MODA, (b) $k-\varepsilon$ MODB.

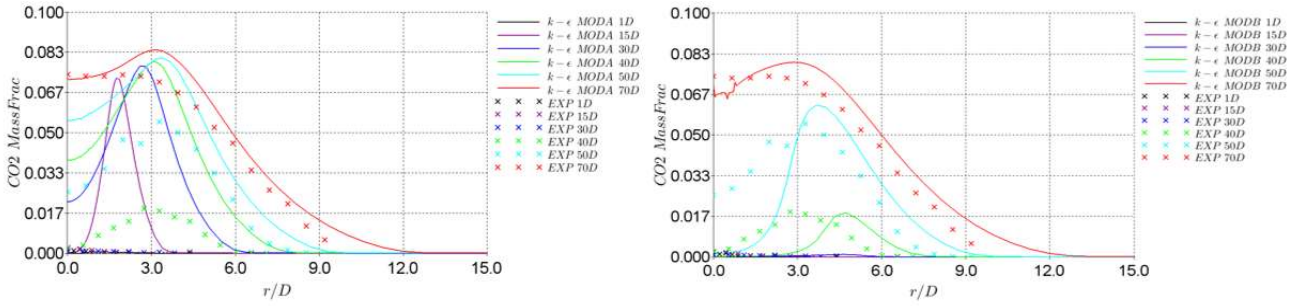

(a) **(b)**

Figure 10. CO2 Mass fraction profiles: (a) $k-\varepsilon$ MODA, (b) $k-\varepsilon$ MODB.

5. Conclusions

This study analyses the performance of RANS simulations for a turbulent fuel jet development, and its impact on a auto-igniting methane-air flame.

The results obtained using a two-equation turbulence model are compared with experimental data to validate and improve the model accuracy.

The standard $k-\varepsilon$ model with C_μ equal to 0.09 shows a significant over-diffusion in the non-reactive jet simulations, which has the root cause in the overprediction of the shear stress in the initial region.

The proposed modified $k-\varepsilon$ with C_μ 0.03 and σ_k 0.75 reduces these effects, resulting in more accurate velocity and turbulence fields.

In the reactive jet simulations, the standard $k-\varepsilon$ causes early ignition and incorrect flame development. The modified $k-\varepsilon$ model with the default EDC shows an expected late ignition due to a reduction of the reaction rate.

Based on a sensitivity study, a consistent modification of the EDC model constant C_γ to 2.3, allows to achieve more accurate flame ignition and development prediction.

The results address the importance of properly modelling the jet flow establishment region, in order to obtain an accurate prediction of auto-igniting diffusion flames and turbulent jet flows in general.

Acknowledgements

This research was developed within the project “Network 4 Energy Sustainable Transition – NEST” funded under the National Recovery and Resilience Plan (NRRP), Mission 4 Component 2 Investment 1.3 - Call for tender No. 1561 of 11.10.2022 of Ministero dell’Università e della Ricerca (MUR); funded by the European Union – NextGenerationEU.

References

[1] Weber R., Gupta A. K., Mochida S., High temperature air combustion (HiTAC): How it all started for applications in industrial furnaces and future prospects, Applied Energy, 278, 2020.
[2] Mcallister S., Chen J.-Y., Pello-Fernandez A. C., Fundamentals of Combustion Processes, Springer, 2011.
[3] Dally, B.B., Karpetis, A.N., Barlow, R.S., Structure of turbulent non-premixed jet flames in a diluted hot coflow, Proceedings of the Combustion Institute, 29, 2002, 1147-1154.
[4] Christo, F., Dally, B.B., Modeling turbulent reacting jets issuing into a hot and diluted coflow, Combustion and Flame,142,2005,117-129.
[5] J. Aminian, C. Galletti, S. Shahhosseini, L. Tognotti, Key modeling issues in prediction of minor species in diluted-preheated combustion conditions, Applied Thermal Engineering, Volume 31, Issue 16, 2011, Pages 3287-3300,
[6] Parente, A., Sadiki, A., Cuoci, A., Zhiyi, L., Comprehensive numerical study of the Adelaide Jet in Hot-Coflow burner by means of RANS and detailed chemistry, Energy, 139, 2017, 555-570.
[7] Li Z., Ferrarotti M., Cuoci A., Parente A., Finite-rate chemistry modelling of non-conventional combustion regimes using a Partially-Stirred Reactor closure: Combustion model formulation and implementation details, Applied Energy, Volume 225, 2018, Pages 637-655.
[8] Oldenhof E., Tummers M.J., van Veen E.H., Roekaerts D.J.E.M., Ignition kernel formation and lift-off behaviour of jet-in-hot-coflow flames (2010) Combustion and Flame, 157 (6), pp. 1167 – 1178.
[9] Oldenhof, A., Ashoke D., Sathiah P., Roekaerts D., Numerical Simulation of Delft-Jet-in-Hot-Coflow (DJHC) Flames Using the Eddy Dissipation Concept Model for Turbulence–Chemistry Interaction, Flow Turbulence Combustion, 2011, 87, 537-567.
[10] Lewandowski, MT, Ertesvåg, IS, Analysis of the Eddy Dissipation Concept formulation for MILD combustion modelling, Fuel, Volume 224, 2018, Pages 687-700.
[11] Lewandowski, MT, Ertesvåg, IS, The impact of the fine structure reactor formulation in the Eddy Dissipation Concept for MILD combustion modelling, Proceedings of the 11th ERCOFTAC Engineering, Turbulence, Modelling and Measurement, Palermo, Italy, 21, 23, 2016.
[12] J.W. Labahn, D. Dovizio, C.B. Devaud, Numerical simulation of the Delft-Jet-in-Hot-Coflow (DJHC) flame using Conditional Source-term Estimation, Proceedings of the Combustion Institute, Volume 35, Issue 3, 2015,
[13] Cabra, R., Turbulent Jet Flames Into a Vitiated Coflow, NASA/CR-2004-212887.
[14] Cabra, R., Myrhvold, T., Chen, J.-Y. , Dibble, R.W., Karpetis, A.N., Barlow, R.S., Simultaneous Laser Raman-Rayleigh-LIF Measurements and Numerical Modeling Results Of a Lifted Turbulent H2/N2 Jet Flame In a Vitiated Coflow, Proceedings of the Combustion Institute, Volume 29, 2002/pp. 1881–1888.
[15] R. Cabra, J.-Y. Chen, R.W. Dibble, A.N. Karpetis, R.S. Barlow, Lifted methane–air jet flames in a vitiated coflow, Combustion and Flame, Volume 143, Issue 4, 2005.
[16] Masri, A.R., Wu, Z., Bilger, R.W., An Experimental Investigation of the Turbulence Structure of a Lifted H2/N2 Jet Flame in a Vitiated Co-Flow, Flow, Turbulence and Combustion, 2006.
[17] Gordon, R. L., Stårner, S. H., Masri, A. R. and Bilger, R. W., Further Characterisation of Lifted Hydrogen and Methane Flames Issuing into a Vitiated Coflow, 5th Asia-Pacific Conference on Combustion, 2005
[18] Masri, A.R., Cao, R., Pope, S.B., Goldin, G.M. PDF calculations of turbulent lifted flames of H2/N2 fuel issuing into a vitiated co-flow Combustion Theory and Modelling, 8 (1), pp. 1-22,2004.
[19] Cao R.R., Pope S.B., Masri A.R., Turbulent lifted flames in a vitiated coflow investigated using joint PDF calculations (2005), Combustion and Flame, 142 (4), pp. 438 – 453.
[20] Gkagkas, K., & Lindstedt, R. P. (2009). The impact of reduced chemistry on auto-ignition of H_2 in turbulent flows. Combustion Theory and Modelling, *13*(4), 607–643.
[21] Benim, Ali C., Pfeiffelmann, Björn, Comparison of Combustion Models for Lifted Hydrogen Flames within RANS Framework, Energies, 2020, 13, 152.
[22] Gkagkas, K., Lindstedt, R.P., Transported PDF modelling with detailed chemistry of pre- and auto-ignition in CH4/air mixtures, Proceedings of the Combustion Institute, 31, 2007, 1559-1566.
[23] Ansys Fluent Theory Guide.
[24] http://combustion.berkeley.edu/drm/
[25] http://combustion.berkeley.edu/gri_mech/
[26] Launder, Brian Edward, and Dudley Brian Spalding. *Lectures in Mathematical Models of Turbulence*. London: Academic Press, 1972. Print.
[27] Thangam, S., Analysis of two-equation turbulence models for recirculating flows, NASA/CR-1991-187607.
[28] Kim J, Moin P, Moser R. Turbulence statistics in fully developed channel flow at low Reynolds number. *Journal of Fluid Mechanics*. 1987;177:133-166.

[29] Abid, R., Speziale C. G.; Predicting equilibrium states with Reynolds stress closures in channel flow and homogeneous shear flow. *Phys. Fluids* 1 July 1993; 5 (7): 1776–1782.
[30] Spalart PR. Direct simulation of a turbulent boundary layer up to Rθ = 1410. *Journal of Fluid Mechanics*. 1988.
[31] Tavoularis S, Karnik U. Further experiments on the evolution of turbulent stresses and scales in uniformly sheared turbulence. *Journal of Fluid Mechanics*. 1989;204:457-478
[32] Lee MJ, Kim J, Moin P. Structure of turbulence at high shear rate. Journal of Fluid Mechanics. 1990
[33] McGuirk, J.J., Rodi, W., The Calculation of Three-Dimensional Turbulent Free Jets, Turbulent Shear Flows, 1979,
[34] Pope, S. B., An explanation of the turbulent round-jet/plane-jet anomaly, AIAA Journal, 16,2017, 279-281.
[35] Amielh M., T. Djeridane T., Anselmet F., Fulachier L., Velocity near-field of variable density turbulent jets, International Journal of Heat and Mass Transfer, Volume 39, Issue 10, 1996, Pages 2149-2164.
[36] Wang P., Fröhlich J., Michelassi V., Rodi W., Large-eddy simulation of variable-density turbulent axisymmetric jets, International Journal of Heat and Fluid Flow, Volume 29, Issue 3, 2008, Pages 654-664.
[37] Gran, I.R., Magnussen, B.F. (1996) A Numerical Study of a Bluff-Body Stabilized Diffusion Flame. Part 2. Influence of Combustion Modeling And Finite-Rate Chemistry, Combustion Science and Technology, 1996, 119, 191-217.
[38] Estersvag, I.S., Magnussen, B.F., The Eddy Dissipation Turbulence Energy Cascade Model, Combustion Science and Technology, 1999.
[39] Jimenez, J., Hoyas, S., Simens, M.P., Mizuno, Y., Turbulent boundary layers and channels at moderate Reynolds numbers, Journal of Fluid Mechanics, 657, 2010, 335-360.